SLAC-PUB-4261
SCIPP-87/90
NSF-ITP-87-53
May 1987
T/E/AS

Neutrino Mixing, Decays and Supernova 1987A*

JOSHUA A. FRIEMAN

Stanford Linear Accelerator Center

Stanford University, Stanford, California, 94305

HOWARD E. HABER

Santa Cruz Institute for Particle Physics

University of California, Santa Cruz, California 95064

and

KATHERINE FREESE

Institute for Theoretical Physics

University of California, Santa Barbara, California 93106

Submitted to *Physics Letters B*

*Work supported by the Department of Energy, contract DE–AC03–76SF00515, and the National Science Foundation, Supplemented by funds from the National Aeronautics and Space Administration.

ABSTRACT

We discuss the evolution of neutrino beams in the presence of both flavor mixing and decays, and we comment on the implications of the supernova 1987A observations for neutrino mixings and lifetimes. Although the implied stability of the electron neutrino severely constrains particle physics models with neutrino decay, it may not rule out the possibility that neutrino decay accounts for the discrepancy between the observed and expected solar neutrino flux.

Recently, the observation[1,2] of electron (anti-)neutrinos from a supernova in the large magellanic cloud has been reported. Since the gross features of the neutrino emission from Type II supernovae are thought to be insensitive to the details of theoretical collapse models, it may be possible to use supernovae as pulsed sources for a very long beam (tens of kpc) neutrino laboratory. In principle, one could derive information about the properties of neutrinos from all aspects of the supernova neutrino signal, i.e., from the overall signal strength, its spectrum, and its time dependence. However, the time structure of the neutrino luminosity is determined in part by the detailed mechanisms of stellar core bounce and envelope ejection[3]. These processes are not completely understood, but they may depend sensitively on the progenitor star's mass and angular momentum. For example, in numerical simulations of stars of mass $M \gtrsim 16M_{\odot}$, the shock wave stalls on its way out of the collapsed core, and envelope ejection is delayed for of order 0.6 sec[4]. In these models, the neutrino signal shows a pulsed structure not seen in lower mass stars[5]. In addition, the ν pulse may be drawn out due to rotation[6] or by non-zero neutrino masses ($\gtrsim O(eV)$)[7,8]. Although interesting, these effects may be difficult to disentangle until the theory of supernova collapse is on firmer ground.

By contrast, the energetics of the collapse, and, therefore, the broad features of the consequent neutrino flux appear to be fairly model independent. Essentially, the binding energy of the resultant neutron star or black hole, of order a few times 10^{53} ergs, must be released during the collapse, the bulk of it in the form of neutrinos. We will focus on what can be learned about neutrinos from only these general aspects of the collapse[$3-5$,9]. In particular, we will be mainly interested in neutrinos lighter than $O(eV)$, for which large mixing angles

are experimentally allowed[10]. Neutrino masses in this range play no significant role in the time structure of the neutrino signal from SN 1987A.

Although the neutronization of the core produces an initial short burst of electron neutrinos, the bulk of the neutrinos ($\gtrsim 90\%$) are expected to come from pair emission, $e^+ + e^- \rightarrow \nu_i + \bar{\nu}_i$. This dominant process produces light neutrinos of all flavors, due to both charged and neutral currents, and will be the focus of our consideration in this paper. Initially, the core density is sufficiently high, $\rho \geq 2 \times 10^{11} gm/cm^3$, that the matter behind the shock front is opaque to neutrinos. The trapped neutrinos reach approximate thermal equilibrium in the core and leak out on a diffusion time of order $1 - 2$ sec. (Half of the total neutrino energy is emitted in the first second or so; the remaining half, carried by less energetic neutrinos, is emitted over the next few tens of seconds[5].)

The neutrino spectrum is determined by the temperature in the 'neutrinosphere', where the neutrino optical depth approaches unity. For electron neutrinos, the average energy in the neutrinosphere is of order[3,5,9] $\bar{E}_{\nu_e} \simeq 10 - 12 MeV$, while for electron anti-neutrinos, in the first 0.5 sec of the burst, $\bar{E}_{\bar{\nu}_e} \simeq 12 - 15 MeV$, rising by a few MeV subsequently. Since ν_μ, ν_τ only interact via neutral currents, their mean free paths are longer, so their energies are characteristic of the higher temperatures deeper in the core, $\bar{E}_{\nu_\mu, \nu_\tau} \simeq 20 - 23 MeV$. (These average energies all depend slightly on the progenitor iron core mass.) Also, since the mean free path scales as E_ν^{-2}, low energy neutrinos can escape from deeper, hotter regions. As a result, the neutrino spectra are not purely thermal, falling more rapidly at higher energies than Fermi-Dirac spectra with the average energies given above. Reasonable fits to the high energy parts of the time-integrated spectra found numerically in ref.5 are obtained by taking Fermi-

Dirac spectra (with zero chemical potential) with $T_{\nu_e} = 3.5MeV$, $T_{\bar{\nu}_e} = 4MeV$ (solid curve in Fig.1), and $T_{\nu_\mu,\nu_\tau} = 7MeV$. We have fit the high energy portion of the spectrum because this is the most important in terms of detection; these fits underestimate the average neutrino energy($\bar{E}_\nu = 3.15T_\nu$) by only $1-2MeV$.

Over the energy range of interest, $E_\nu \simeq 10-40MeV$, the interaction rate of $\bar{\nu}_e$ in water Cerenkov detectors such as IMB and Kamiokande II is at least 10 times higher than for ν_e; $\nu_{\mu,\tau}$ rates are down by an additional factor of 6 from ν_e. Since supernova theory suggests roughly equal numbers of ν_e and $\bar{\nu}_e$ will be produced, we assume the large majority of observed events is due to $\bar{\nu}_e$ absorption on free protons. For simplicity, we will focus on the data of ref.1; inclusion of the IMB data does not substantially change the results.

First consider the case of no neutrino mixing or decay. The number of expected $\bar{\nu}_e$ events in the Kamiokande detector is given by

$$N_{det} = \frac{N_{\bar{\nu}}^{SN} N_p}{4\pi R^2} \int_0^\infty \epsilon(E_{\bar{\nu}}) \sigma_{\bar{\nu}}(E_{\bar{\nu}}) f(E_{\bar{\nu}}) dE_{\bar{\nu}} \qquad (1)$$

where $f(E_{\bar{\nu}})$ is a normalized Fermi-Dirac distribution with $T_{\bar{\nu}_e} = 4MeV$ ($\int f(E)dE = 1$), $\epsilon(E)$ is the Kamiokande detector efficiency[1] which we have fit with the function $\epsilon(E) = 1 - e^{-(E/10MeV)^2}$, and the $\bar{\nu}_e$ absorption cross-section is given by[11] $\sigma_{\bar{\nu}_e} = 9.7 \times 10^{-44}[(E_\nu/MeV) - 1.29]^2 cm^2$. In Fig.2, the solid curve shows the distribution of expected $\bar{\nu}_e$ events in the Kamiokande detector, proportional to the integrand of Eqn.1. Within the experimental uncertainties, this curve is consistent with the observed Kamiokande II event distribution from SN 1987A. In the coefficient of the integral, $R = 1.5 \times 10^{23} cm$ is the distance to the LMC, $N_p = (1/9)(2.14 \times 10^9 gm/m_p)$ is the number of free protons in the fiducial

volume of the detector, and $N_{\bar{\nu}}^{SN}$ is the total number of electron antineutrinos emitted by the supernova in the first few seconds, assuming a static spectrum. Given the number of observed $\bar{\nu}_e$ events in the Kamiokande detector[1] (which we take to be $10N_{10}^{det}$), we can use Eqn.1 to find the amount of energy released in the form of electron antineutrinos, $E_{\bar{\nu}_e}^{SN} = 3.15T_{\bar{\nu}_e}N_{\bar{\nu}_e}^{SN}$. Assuming that $\simeq 18\%$ of the released energy is in the form of $\bar{\nu}_e$[5], we infer a *total* energy release (over the first few seconds) of $E_{SN} \simeq (2.5 \pm 0.8)N_{10}^{det} \times 10^{53}$ ergs from the $\bar{\nu}_e$ signal, assuming no mixing or decay. (The quoted uncertainty is the 1σ statistical error in counting rate.) We emphasize that this is a lower bound on the total energy release of the supernova, arrived at by assuming all of the emitted energy is in the form of prompt neutrinos; the actual energy release depends on the fraction of energy emitted after the first few seconds (at undetectably low energies), but should be less than a factor two higher than this. This estimate is in good agreement with what one would expect in the collapse of a $1.4M_{\odot}$ Fe core to a $1.3M_{\odot}$ neutron star[5].

We now consider the effects of neutrino mixing and decay on the $\bar{\nu}_e$ signal of supernovae. Although our discussion will be more general, our primary motivation is the suggestion by Bahcall and collaborators[12,13] that ν_e decay in flight from the sun may explain the solar neutrino problem. The idea of such fast neutrino decays may be theoretically natural in the context of extended Majoron models[13 – 17]. At first sight, our study appears quixotic: a $\nu_e(\bar{\nu}_e)$ lifetime (at $E_\nu \simeq 10MeV$) of order the 500 sec transit time from the sun to the earth clearly conflicts with the observation of electron antineutrinos from the LMC, 160,000 light years away. In fact, the observation of neutrinos of energy $\simeq 10MeV$ from SN 1987A gives a lower bound on the ν_e lifetime,

$\tau_{\nu_e} > 5 \times 10^5 (m_{\nu_e}/eV)$ sec, while the lifetime of interest for the solar neutrino problem is[13] $\tau_{\nu_e} \simeq 5 \times 10^{-5} (m_{\nu_e}/eV)$ sec. (For ν_e decay to a massless neutrino and massless pseudoscalar at tree level, with laboratory rate $\Gamma = g^2 m_{\nu_e}^2 / 16\pi E_{\nu_e}$, the lower bound on the ν_e lifetime from the supernova corresponds to an upper limit on the coupling constant, $g < 2.6 \times 10^{-10} (m_{\nu_e}/eV)^{-1}$.) However, this argument neglects the importance of ν flavor mixing, which is generally present in models in which neutrino decay occurs. It turns out that, in the case of relatively large mixing angles, neutrino decay does not drastically reduce the $\bar{\nu}_e$ detection rate from SN 1987A, and may be consistent with expectations from supernova theory. Furthermore, such large mixings do *not* play havoc with the neutrino decay solution of the solar neutrino problem.

To simplify the discussion, let us consider a model with mixing between two neutrino flavors, ν_e and, say, ν_μ. These weak eigenstates are mixtures of the mass eigenstates ν_1, ν_2, with masses m_1, $m_2 > m_1$:

$$\begin{pmatrix} |\nu_1\rangle \\ |\nu_2\rangle \end{pmatrix} = \begin{pmatrix} \cos\theta & -\sin\theta \\ \sin\theta & \cos\theta \end{pmatrix} \begin{pmatrix} |\nu_e\rangle \\ |\nu_\mu\rangle \end{pmatrix} \tag{2}$$

In order to consider the case where ν_2 is unstable to non-radiative decay, we must generalize the standard neutrino mixing formalism to allow for a finite neutrino lifetime. In this case, it is convenient to let θ run from 0° to 90°, with angles near 45° denoting large mixing between ν_e and ν_μ. Two possibilities will be considered: either $\nu_2 \to \nu_1 \phi$ or $\nu_2 \to \bar{\nu}_1 \phi$, where ϕ is a light (pseudo)scalar, carrying lepton number $L = 0$ or 2. Suppose we start with a state at $t = 0$ given by

$$|\psi(0)\rangle = |\tilde{\nu}\rangle = \cos\alpha |\nu_e\rangle + \sin\alpha |\nu_\mu\rangle \tag{3}$$

with momentum p. Then, at later times, the state is

$$|\psi(t)\rangle = e^{-iE_1 t}\cos(\theta+\alpha)|\nu_1\rangle + e^{-iE_2 t}\sin(\theta+\alpha)|\nu_2\rangle + \sum_k c_k(t)|k\rangle \qquad (4)$$

where, for $p \gg m_1, m_2$, we have $E_1 = p + m_1^2/2p$, $E_2 = p + m_2^2/2p - i\Gamma/2$, and the decay rate (in the lab frame) is $\Gamma = m_2/(E_2\tau)$. The continuum of states represented by the ν_2 decay products are $|k\rangle = |\nu_1\phi\rangle$ or $|\bar{\nu}_1\phi\rangle$ of appropriate final state momenta.

Inserting Eqn.2 into Eqn.4, we may easily compute the probabilities P that the state at time t will be observed as either ν_e, ν_μ, or $|k\rangle$ (in the latter case, we integrate over the allowed final state phase space). In obvious notation,

$$\begin{aligned} P_{\tilde{\nu}\to\nu_\mu} = {} & \cos^2(\theta+\alpha)\sin^2\theta + e^{-\Gamma t}\sin^2(\theta+\alpha)\cos^2\theta \\ & - \frac{1}{2}e^{-\Gamma t/2}\sin 2\theta \sin 2(\theta+\alpha)\cos\left[\frac{(m_2^2-m_1^2)t}{2p}\right] \end{aligned} \qquad (5)$$

$$P_{\tilde{\nu}\to\nu_e} + P_{\tilde{\nu}\to\nu_\mu} = \cos^2(\theta+\alpha) + e^{-\Gamma t}\sin^2(\theta+\alpha) \qquad (6)$$

Since the sum of all probabilities must be 1,

$$\sum_k P_{\tilde{\nu}\to|k\rangle} = (1-e^{-\Gamma t})\sin^2(\theta+\alpha) \qquad (7)$$

At the detector, $\nu_1(\bar{\nu}_1)$ will be observed as either $\nu_\mu(\bar{\nu}_\mu)$ or $\nu_e(\bar{\nu}_e)$ according to Eqn.2. We emphasize that the decay-product neutrinos are incoherent with respect to other neutrinos in the primary beam which have not decayed. Thus,

$$\sum_k P_{\tilde{\nu}\to|(\nu_e \text{or} \bar{\nu}_e)\phi\rangle} = (1-e^{-\Gamma t})\sin^2(\theta+\alpha)\cos^2\theta \qquad (8)$$

and

$$\sum_k P_{\tilde{\nu}\to|(\nu_\mu or \bar{\nu}_\mu)\phi\rangle} = (1-e^{-\Gamma t})\sin^2(\theta+\alpha)\sin^2\theta. \tag{9}$$

In applying Eqns.5 – 9, we assume that the oscillation length is much smaller than astronomical distances, so the term proportional to $\cos(m_2^2 - m_1^2)t/2p$ will average to zero.

In this paper, these formulae will be applied by setting $\alpha = 0$ or $\alpha = 90°$, corresponding to an initially produced ν_e or ν_μ. If the MSW effect[18, 19] is operative, an initially produced weak interaction eigenstate can emerge from the star as a linear combination of ν_e and ν_μ due to resonant oscillations in matter. When we consider the MSW effect, we will assume a small vacuum mixing angle and that resonant mixing is complete for the neutrino energy range of interest, so that again $\alpha \simeq 0°$ or $90°$. Finally, we note that, although the above discussion has been couched in terms of initially produced neutrinos, the formalism goes through unchanged for initially produced antineutrinos.

In computing the energy spectrum of the neutrinos $\nu_1(\bar{\nu}_1)$ which result from ν_2 decay, we make one further simplification by taking ϕ to be massless (as in the Majoron model[14 – 17]). Then, the $\nu_1(\bar{\nu}_1)$ energy E_1 must kinematically satisfy $E_1^- \leq E_1 \leq E_1^+$, where

$$E_1^\pm = \frac{E_2(m_1^2+m_2^2) \pm p_2(m_2^2-m_1^2)}{2m_2^2}. \tag{10}$$

For $E_2 \gg m_2$, $E_1^+ \simeq E_2$ and $E_1^- \simeq E_2 m_1^2/m_2^2$. To compute the energy spectrum of ν_1 in the laboratory, we must know its angular distribution in the ν_2 rest frame. Since ν_2 is produced and ν_1 is detected via standard weak interaction processes, both ν_1 and ν_2 are left-handed. The angular distribution of ν_1 in the

ν_2 rest frame is then easily computed to be proportional to $\cos^2(\theta_1^*/2)$, where θ_1^* is the decay angle of ν_1 with respect to the laboratory three-momentum of ν_2. For $\nu_2 \to \bar{\nu}_1\phi$, the detected $\bar{\nu}_1$ is right-handed, so the corresponding angular distribution is proportional to $\sin^2(\theta_1^*/2)$. The resulting energy distributions in the laboratory frame are obtained by relating θ_1^* with E_1. The results are

$$\begin{aligned} \cos^2\frac{\theta_1^*}{2} &= \frac{m_2^2(E_1 - E_1^-)}{p_2(m_2^2 - m_1^2)} \\ \sin^2\frac{\theta_1^*}{2} &= \frac{m_2^2(E_1^+ - E_1)}{p_2(m_2^2 - m_1^2)} \end{aligned} \tag{11}$$

where $E_1^{\pm}$ are defined in Eqn.10. Thus, the energy spectrum of $\nu_1(\bar{\nu}_1)$ is linear in E_1 (for fixed E_2). This applies to both the spectrum of decay products of a single ν_2 beam averaged over decay angles, and to the spectrum seen at the detector which arises from summing over different initial ν_2 beam directions.

Let us apply this formalism to find the flux of $\bar{\nu}_e$ at the detector from a distant source of both neutrino flavors. To find the neutrino signal at the earth, we must fold in these results with the initial neutrino energy spectra discussed earlier. For the case $\nu_2 \to \bar{\nu}_1\phi$, the $\bar{\nu}_e$ spectrum at the detector is (assuming no MSW mixing for the moment)

$$\begin{aligned} f_{\bar{\nu}_e}^{det}(E) \propto\ & N_{\bar{\nu}_e} f_{\bar{\nu}_e}(E)(\cos^4\theta + \sin^4\theta e^{-t\Gamma(E)}) \\ & + N_{\bar{\nu}_\mu} f_{\bar{\nu}_\mu}(E)\sin^2\theta\cos^2\theta(1 + e^{-t\Gamma(E)}) \\ & + \left(1 - \frac{m_1^2}{m_2^2}\right)^{-2} \int_E^{E(\frac{m_2}{m_1})^2} \frac{dE_2}{E_2^2}(1 - e^{-t\Gamma(E_2)})(E_2 - E) \\ & \times 2[N_{\nu_e}\sin^2\theta\cos^2\theta f_{\nu_e}(E_2) + N_{\nu_\mu}\cos^4\theta f_{\nu_\mu}(E_2)] \end{aligned} \tag{12}$$

where we have used Eqns.5 – 11, with $\alpha = 0$ for initially produced ν_e and $\alpha = \pi/2$ for initially produced ν_μ. Here, $f_{\nu_i}(E)$ is the normalized neutrino spectrum at the source, and N_{ν_i} is the total number of emitted neutrinos of flavor i. For the alternative case, $\nu_2 \to \nu_1\phi$, in the last term f_{ν_e}, f_{ν_μ} are replaced by $f_{\bar{\nu}_e}$, $f_{\bar{\nu}_\mu}$, and the factor $(E_2 - E)$ is replaced by $(E - E_2(m_1/m_2)^2)$. This last feature can be understood in terms of angular momentum conservation, by analogy with pion decay: in ν_2 decay, the emission of $\bar{\nu}_1$ along the ν_2 beam direction, which corresponds to $E_1 = E_1^+ \simeq E_2$, is forbidden, while the emission of ν_1 is forbidden in the backwards direction.

In Figure 1 we plot both the spectrum of $\bar{\nu}_e$ emitted by the supernova (solid curve, $f^{det}_{\bar{\nu}_e} = N_{\bar{\nu}_e} f_{\bar{\nu}_e}(E)$), and the modified $\bar{\nu}_e$ spectrum at the detector (from Eqn.12) for various mixing angles. We have assumed a decay time short compared with the transit time from the LMC, so all terms with $e^{-\Gamma t}$ are dropped. From ref.5, the total numbers of emitted neutrinos are taken in the ratio $N_{\nu_e} : N_{\bar{\nu}_e} : N_{\nu_\mu} : N_{\bar{\nu}_\mu} = 2 : 1.4 : 1 : 1$. For definiteness, we have also taken a $\nu_e - \nu_\mu$ mass matrix of the form[13] $\begin{pmatrix} M & m \\ m & 0 \end{pmatrix}$; the eigenvalues of this matrix are denoted by m_1 and m_2 as before. By definition, $m_2 > m_1$ so that $\tan^2\theta = (m_1/m_2)$ for $\theta < 45°$ and $\tan^2\theta = (m_2/m_1)$ for $\theta > 45°$. Except for θ near $45°$, the results are insensitive to this final assumption. In Majoron models, the neutrino mass parameters m and M depend on vacuum expectation values of various scalar fields and unknown Yukawa couplings. Thus, the mixing angles in these models are fairly unconstrained and may be quite large.

In Fig.2, we show the expected distribution of $\bar{\nu}_e$ events in the Kamiokande detector (see Eqn.1) for various mixing angles (dashed and dotted curves), compared with the case of no mixing or decay discussed above (solid curve). We show

the case $\nu_2 \rightarrow \bar{\nu}_1\phi$; for most mixing angles, the results for this case are nearly indistinguishable from the decay $\nu_2 \rightarrow \nu_1\phi$. For decays relevant for the solar neutrino problem, the parameter range of interest is $45° < \theta < 90°$, for which the unstable mass eigenstate ν_2 mixes predominantly with ν_e. As $\theta \rightarrow 90°$, i.e., for ν_e (and $\bar{\nu}_e$) unstable, the $\bar{\nu}_e$ signal drops as expected. As θ is reduced from 90° to 45°, i.e., as the admixture of ν_μ to the decaying eigenstate is increased, the number of $\bar{\nu}_e$ events seen by the detector grows to become comparable with that of the pristine supernova $\bar{\nu}_e$ spectrum. For $\theta \lesssim 50°$, the $\bar{\nu}_e$ signal is actually *enhanced* by ν_μ decay. (Recall that $\theta = 0°$ corresponds to pure ν_μ decay.) Note that in all cases the electron antineutrino energy spectrum becomes harder due to mixing with the higher energy ν_μ's.

For completeness, in Fig.3 we show the expected event distribution in the case of mixing without decay (in this case, for pure vacuum mixing, θ and $90° - \theta$ give the same result). The curve marked 'MSW' corresponds to resonant $\bar{\nu}_e - \bar{\nu}_\mu$ mixing ($\alpha = 90°$ for initially produced $\bar{\nu}_e$ and $\alpha = 0$ for initially produced $\bar{\nu}_\mu$) and $\theta \simeq 90°$. In this case, the $\bar{\nu}_e$ and $\bar{\nu}_\mu$ distributions are simply interchanged in the supernova envelope, so the $\bar{\nu}_e$ spectrum at the detector corresponds to the neutrinosphere ν_μ spectrum. Note that for θ near 90°, i.e., in the case where the heavier eigenstate ν_2 is predominantly ν_e, only antineutrinos undergo the MSW effect[18]; the alternative case of resonant $\nu_e - \nu_\mu$ oscillations for small θ has been discussed by Walker and Schramm[19].

Table 1 shows the inferred supernova burst energies from the Kamiokande data for the various cases. These numbers should be compared with the binding energy of neutron stars and black holes expected to be formed in typical Type II collapse[5], $E_{SN} = (3.0 \pm 1.5) \times 10^{53}$ ergs. (The mass and binding energy of

the remnant are functions of the iron core progenitor mass, and depend on the dynamics of the shock[4].) In the absence of information on the remnant mass, the range $\theta \lesssim 60°$ appears to be consistent with expectations from supernova theory. The MSW case may be marginally consistent with supernova energetics, but it appears to predict a spectrum harder than is observed.

In Fig.4, we show the effects of mixing and decay on the ^8B solar ν_e spectrum. In this case, assuming the sun produces only ν_e, the ν_μ terms in Eqn.12 are absent. For $\nu_2 \rightarrow \bar{\nu}_1\phi$ decay, only the first term in Eqn.12 survives, while for $\nu_2 \rightarrow \nu_1\phi$, there is also a term involving an integration over the ν_e spectrum. The curve marked '^8B' is a fit (good to a few percent) to the undistorted ^8B ν_e spectrum[20]. The ν_2 decay rate in the lab frame is

$$\Gamma(E_2) = \left(\frac{m_2}{E_2}\right) \frac{g^2(m_2 - m_1)^3(m_1 + m_2)}{16\pi m_2^3} \tag{13}$$

where for illustrative purposes we assume, following Gelmini and Valle[16], that the $\nu_1\nu_2\phi$ coupling is purely pseudoscalar. The coupling constant g is chosen so that for $\theta = 90°$ ($m_1 = 0$), corresponding to pure ν_e decay, the decay rate is $\Gamma(E_2, 90°) = (10MeV/E_2)/500$ sec[13]. The lower 60° curve corresponds to $\nu_2 \rightarrow \bar{\nu}_1\phi$ decay, while the upper 60° curve denotes the alternative case, $\nu_2 \rightarrow \nu_1\phi$. The 45° curve corresponds to maximal vacuum oscillations without decay (for the neutrino mass matrix chosen above, the decays are phase space suppressed as $\theta \rightarrow 45°$). For $\theta = 90°$, Bahcall, etal.[13] find the ^{37}Cl capture rate is reduced from the predicted rate of 5.8($\pm$2) SNU (with approximately 4.3 SNU due to ^8B) to the observed value 2.1($\pm$0.3) SNU[21]. For $\theta = 45°$, the predicted rate is reduced to 2.9($\pm$1) SNU, marginally consistent with the observations. There is a large overlap of the range allowed by the supernova observations, $\theta \lesssim 60°$,

with that required to solve the solar neutrino problem with mixing and decay, $\theta \gtrsim 45°$.

We have presented the formalism of neutrino mixing modified to include the non-radiative decay of the heavy mass eigenstate, and have illustrated the combined effects of mixing and decay on the neutrino signals from supernovae and the sun. We have shown that models with neutrino decay and mixing angles $\theta \lesssim 60°$ are difficult to rule out on the basis of SN 1987A alone. Such models with large mixing angles ($45° \lesssim \theta \lesssim 60°$) could also solve the solar neutrino puzzle. (Although large mixing angles are not theoretically favored in most models of neutrino masses, they may not be unnatural in the context of Majoron models, which also provide for neutrino decay.) Our emphasis has been on results which depend as little as possible on particular supernova and particle physics models. Specific models with neutrino decay[14−17] may be constrained on other grounds, for example, by neutrinoless double beta decay experiments[22, 23], from the $Z°$ width[24], and by the effects of neutrino scattering and annihilation on the dynamics of supernovae[25]; this last effect gives an upper bound on the coupling constant[26], $g \lesssim 10^{-5} - 10^{-4}$, which is of order that required to solve the solar neutrino problem with neutrino decay. For certain parameter ranges, such models may also predict other effects on the neutrino signal from supernovae which we have not included, such as the regeneration of the ν_2 beam by scattering on a thermal ϕ background[17]. Finally, we point out that the two-flavor model discussed here can be generalized (in a variety of ways) to include additional neutrino generations.

We thank Andrzej Drukier, David Seckel, Bob Wagoner and especially Georg Raffelt for helpful conversations, and Ron Mayle for communicating the results

of Ref.5 before publication. We also thank Georg Raffelt and David Seckel for pointing out an error in an earlier version of the paper. This research was supported in part by NSF under Grant No.PHY82-17853, supplemented by funds from NASA at Santa Barbara, by DOE contract DE-AC03-76F00515 at SLAC, and by DOE contract DE-AA03-76SF00010 at Santa Cruz.

REFERENCES

1. K. Hirata, et al.,, *Phys.Rev.Lett.* **58** (1987), 1490.
2. R.M. Bionta, et al.,, *Phys.Rev.Lett.* **58** (1987), 1494.
3. D.N. Schramm, R. Mayle and J.R. Wilson, *Nuov.Cim.* **9C** (1986), 443.
4. J.R. Wilson, R. Mayle, S. Woosley and T. Weaver, *Ann.N.Y.Acad.Sci.* **470** (1986), 267.
5. R. Mayle, J.R. Wilson and D.N. Schramm, *Ap.J.*, to appear.
6. R. Mayle, private communication.
7. G.T. Zatsepin, *ZhTEF.Pis.Red.* **8** (1968), 333.
8. T. Piran, *Phys.Lett.* **102B** (1981), 299. P. Reinartz and L. Stodolsky, *Z.Phys.* **C27** (1985), 507.
9. A. Burrows, *Ap.J.* **283** (1984), 848.
10. F. Boehm, in *Neutrino '86*, eds. T. Kitagaki and H. Yuta (World Scientific, Singapore, 1986.)
11. P. Vogel, *Phys.Rev.* **D29** (1984), 1918.
12. J.N. Bahcall, N. Cabibbo and A. Yahil, *Phys.Rev.Lett.* **28** (1972), 316.
13. J.N. Bahcall, S.T. Petcov, S. Toshev and J.W.F. Valle, *Phys.Lett.* **181B** (1986), 369.
14. G.B. Gelmini and M. Roncadelli, *Phys.Lett.* **99B** (1981), 411.
15. J.W.F. Valle, *Phys.Lett.* **131B** (1983), 87.
16. G.B. Gelmini and J.W.F. Valle, *Phys.Lett.* **142B** (1984), 181.
17. S. Nussinov, *Phys.Lett.* **185B** (1987), 171.

18. S.P. Mikhaeyev and A. Yu Smirnov, *Sov.J.Nuc.Phys.* **42** (1985), 913. L. Wolfenstein, *Phys.Rev.* **D17** (1978), 2369; **20** (1979) 2634.

19. T.P. Walker and D.N. Schramm, Fermilab preprint, 1986.

20. J.N. Bahcall and B. Holstein, *Phys.Rev.* **C33** (1986), 2121.

21. J.N. Bahcall, B.T. Cleveland, R. Davis, Jr. and J.K. Roweley, *Ap.J.Lett.* **292** (1985), L79.

22. D.O. Caldwell, etal., UCSB preprint, 1987.

23. F.T. Avignone,III, R.L. Brodzinski, H.S. Miley and J.H. Reeves, University of South Carolina preprint, 1987.

24. V. Barger, T. Han, N.G. Deshpande and R.J.N. Phillips, University of Wisconsin preprint, March 1987.

25. E.W. Kolb, D.L. Tubbs and D.A Dicus, *Ap.J.Lett.* **225** (1982), L57. D.A. Dicus, E.W. Kolb and D.L. Tubbs, *Nuc.Phys.* **B223** (1983), 532.

26. G. Fuller, talk given at the Santa Barbara conference on Solar Neutrinos, April 1987.

Table 1

SN 1987A Burst Energy inferred from $\bar{\nu}_e$ events

	$E_{SN}/10^{53}N_{10}^{det}$ ergs	
Mixing Angle	No Decay	Decay*
0°	2.5 ± 0.8	1.9 ± 0.6
10	2.4 ± 0.7	2.0 ± 0.6
30	1.8 ± 0.5	2.1 ± 0.6
50	-	2.8 ± 0.8
60	-	5.2 ± 1.6
70	-	10.6 ± 3.2
MSW (90)	1.3 ± 0.4	-

*$\nu_2 \rightarrow \bar{\nu}_1\phi$ decay assumed.

FIGURE CAPTIONS

1) Electron antineutrino spectrum from Type II supernova ($T_{\bar{\nu}_e} = 4MeV$, solid curve) and modified spectrum for various mixing angles, assuming $\nu_2 \rightarrow \bar{\nu}_1\phi$ decay. The curves are relatively, but not absolutely normalized. The curve for 0° (not shown) is nearly degenerate with the 10° spectrum.

2) Distribution of expected $\bar{\nu}_e$ events in the Kamiokande detector with neutrino energy. Solid curve is distribution in absence of mixing and decay. Other curves are for various mixing angles, assuming $\nu_2 \rightarrow \bar{\nu}_1\phi$ decay. The ordinate is arbitrary, but the curves are relatively normalized.

3) Electron antineutrino event distribution in the Kamiokande detector for the case of mixing without decay. The curve marked 'MSW' corresponds to resonant $\bar{\nu}_e - \bar{\nu}_\mu$ mixing, with negligible vacuum mixing ($\theta \simeq 90°$); this curve thus shows the detector response to a Fermi-Dirac spectrum with $T_\nu = 7MeV$.

4) Solar ^8B neutrino spectrum (solid curve) and its modification in the presence of mixing and decay. The upper 60° curve corresponds to $\nu_2 \rightarrow \nu_1\phi$ decay while the lower 60° curve denotes $\nu_2 \rightarrow \bar{\nu}_1\phi$ decay.

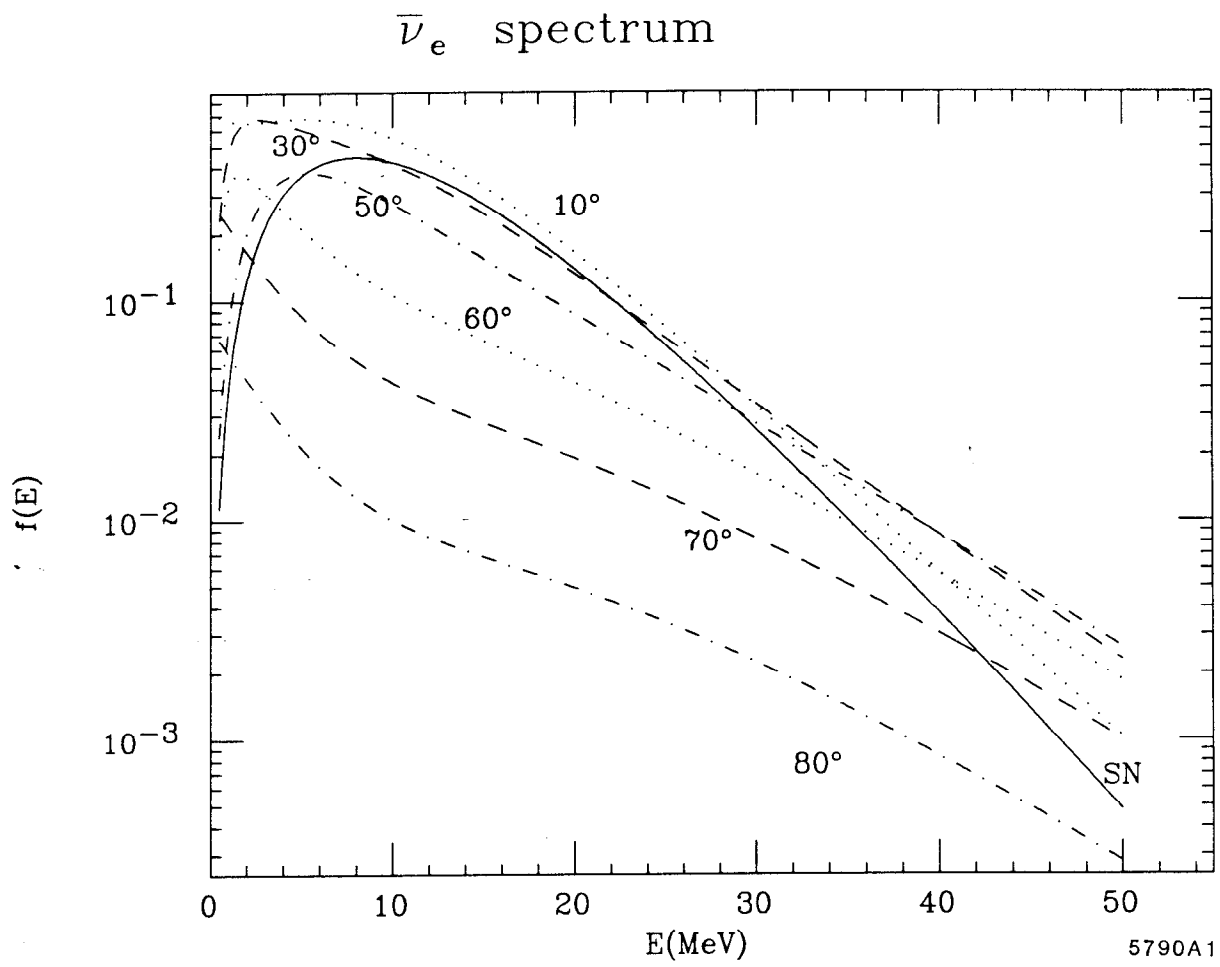
$\bar{\nu}_e$ spectrum
30°
50°
10°
60°
70°
80°
SN
10^{-1}
10^{-2}
10^{-3}
f(E)
0
10
20
30
40
50
E(MeV)
5790A1

Fig. 1

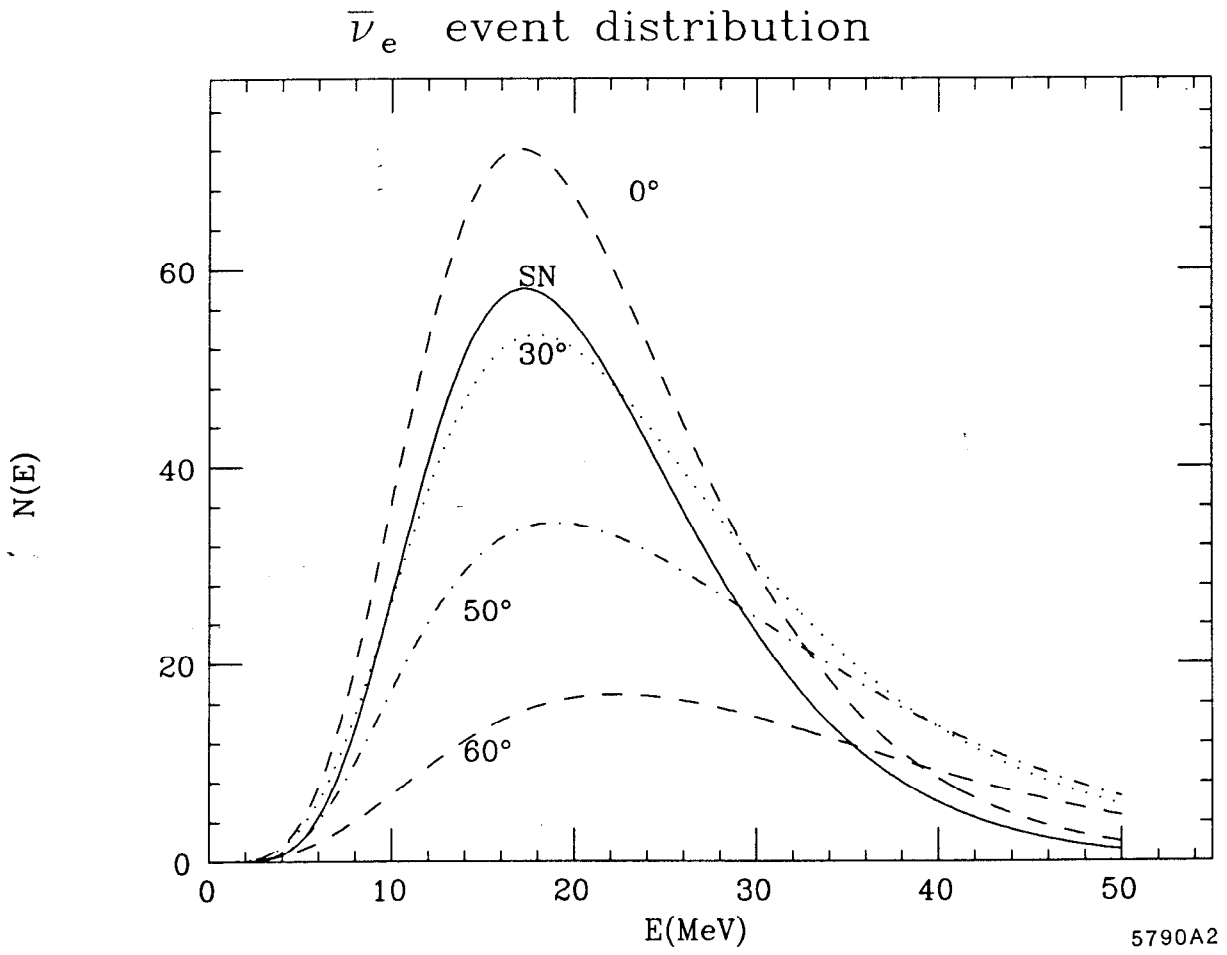
$\overline{\nu}_e$ event distribution
0°
SN
30°
50°
60°
N(E)
E(MeV)
0
10
20
30
40
50
0
20
40
60
5790A2

Fig. 2

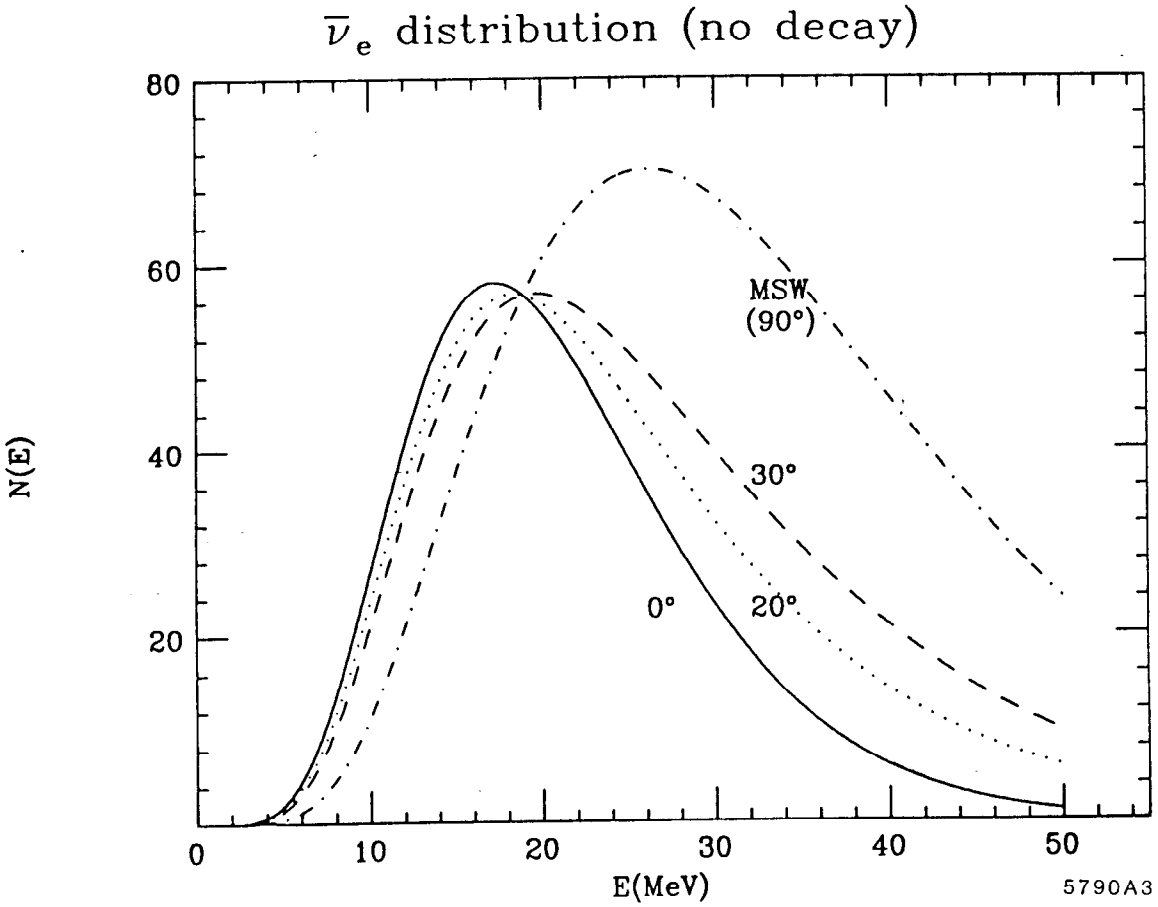
$\overline{\nu}_e$ distribution (no decay)
80
60
40
20
0
10
20
30
40
50
N(E)
E(MeV)
MSW
(90°)
30°
20°
0°
5790A3

Fig. 3

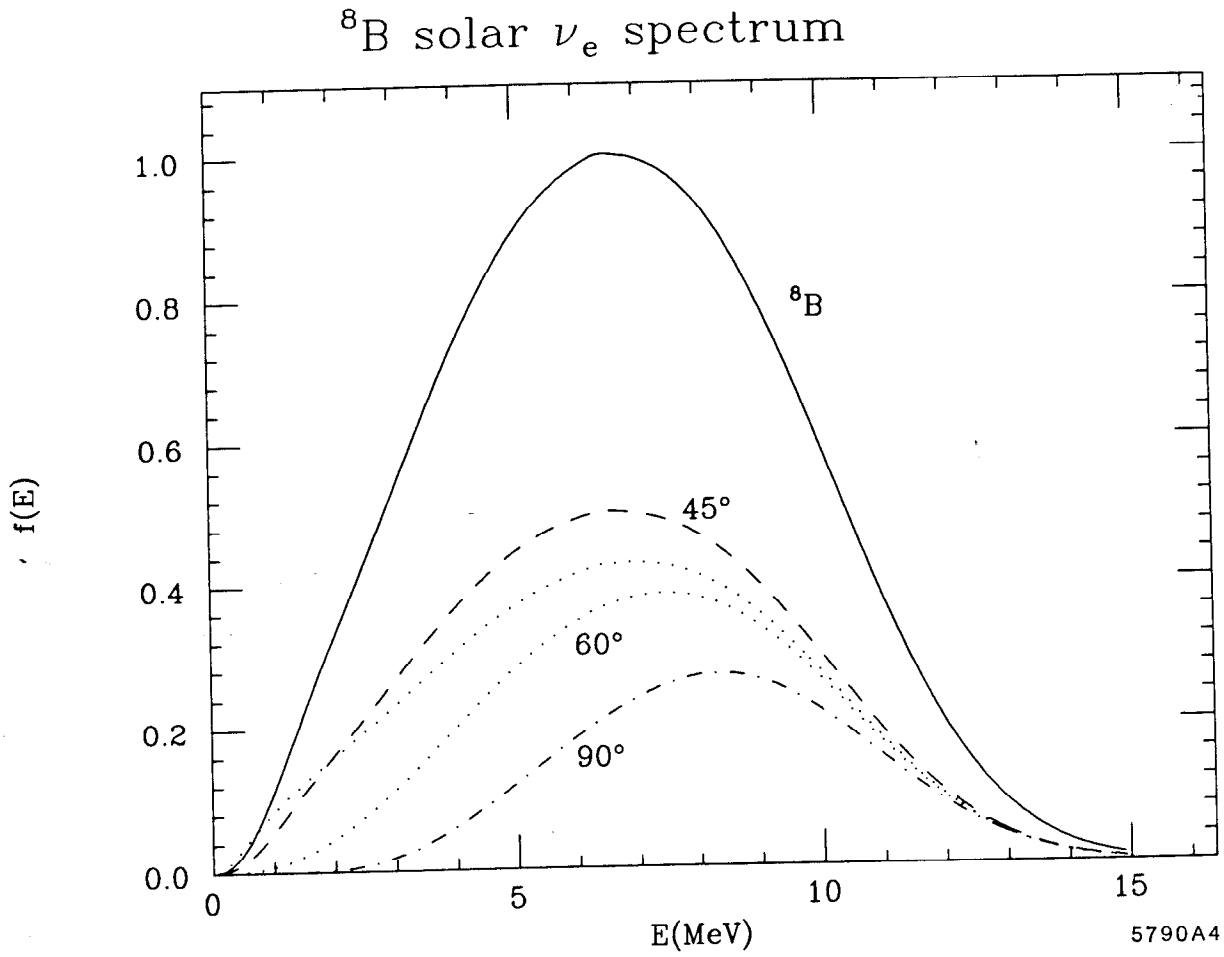
^{8}B solar ν_e spectrum
1.0
0.8
0.6
0.4
0.2
0.0
f(E)
0
5
10
15
E(MeV)
^{8}B
45°
60°
90°
5790A4

Fig. 4